Structural Studies of $(\eta^5\text{-}C_5H_5)_2Nb(SC_6H_5)_2$, $[(\eta^5\text{-}C_5H_5)_2Nb(SC_6H_5)_2^+]$, and $[(\eta^5\text{-}C_5H_5)_2Nb(\mu\text{-}SC_6H_5)_2Mo(CO)_4^+]$

Marcetta Y. Darensbourg,* Rosalice Silva, Joseph Reibenspies, and C. K. Prout†

Department of Chemistry, Texas A&M University, College Station, Texas 77843

Received November 25, 1988

Three related structures have been determined by X-ray crystallography: $Cp_2Nb(SPh)_2$ (1), $[Cp_2Nb(SPh)_2][PF_6]$ (2), and the heterobimetallic $[Cp_2Nb(\mu\text{-}SPh)_2Mo(CO)_4][PF_6]$ (4). The cationic species were obtained upon reactions of the neutral compounds $Cp_2Nb(SPh)_2$ (1) and $Cp_2Nb(\mu\text{-}SPh)_2Mo(CO)_4$ (3) with the one-electron oxidants $[NO][PF_6]$ or $[Fc][PF_6]$. For 1 there are two independent molecules in the unit cell that belongs to the orthorhombic space group *Pbca* with cell parameters a = 13.756 (4) Å, b = 21.532 (6) Å, c = 25.601 (6) Å, and Z = 16. The structure was refined to R = 0.0731 and wR = 0.0931, for 2791 unique observed reflections. Crystals of 2 belong to the monoclinic space group $C2/c$ with cell parameters a = 12.058 (2) Å, b = 16.954 (4) Å, c = 11.079 (2) Å, β = 95.14 (1)°, and Z = 4. The structure was refined to R = 0.0445 and wR = 0.0652 for 1776 uniquely observed reflections. The diamagnetic 4 belongs to the monoclinic space group $C2/c$ with cell parameters a = 33.85 (2) Å, b = 12.409 (4) Å, c = 15.708 (8) Å, β = 96.26 (4)°, and Z = 8. The structure was refined to R = 0.0825 and wR = 0.0930 for 3272 uniquely observed reflections. In all three structures the Nb is in a pseudotetrahedral coordination environment comprised of two Cp rings and the sulfur atoms of the phenylmercapto ligands. The Mo is octahedrally coordinated in 4. The average Nb–S distance varies as follows: for 1, 2.516 (3) Å; for 2, 2.417 (1) Å; for 4, 2.499 (2) Å. The ∠S–Nb–S angle averages to 75.5 (1)° in the Nb(IV) d^1 complex 1 and increases to 101.4 (1)° in the Nb(V) d^0 complex 2. Complexation of $Cp_2Nb(SPh)_2^+$ by $Mo(CO)_4$ hardly changes this angle; in 4 the ∠S–Nb–S is 101.8 (1)° and the ∠S–Mo–S is 103.1 (1)°. The Nb–Mo distance of 3.116 (2) Å in 4 is less than the sum of the covalent radii for Nb and Mo, consistent with the acute angles of 77.7 (1)° for Nb–S(1)–Mo and 77.4 (1)° for Nb–S(2)–Mo. Whereas the Ph groups are in a syn arrangement with respect to the NbS_2 plane in 1, in 2 and 4 they are anti. In solution however variable-temperature ^1H NMR studies of 4 showed a dynamic mixture of syn and anti isomers, with a slight predominance of the anti isomer. Both ν(CO) IR data and cyclic voltammetric studies suggested the positive charge of 4 to be delocalized over both sides of the heterobimetallic complex.

Introduction

The interesting variation of X–M–X angle with electron count in bent metallocenes of formula Cp_2MX_2 (X = one-electron donor ligand) has stimulated theoretical, synthetic, and structural efforts of organometallic chemists for two decades now.[1-5] In cases, the Cp_2MX_2 unit has been noted to bind to another metal center, generating heterobimetallic complexes containing X ligands as bridges, sometimes supported by metal–metal′ bonds. Happening upon the $Cp_2Nb(SPh)_2$ complex, 1, and its derivative heterobimetallic $Cp_2Nb(\mu\text{-}SPh)_2Mo(CO)_4$ (3),[6] we were attracted by the opportunity to examine the effects of both d-electron count and binucleation on the X–Nb–X angle. Additionally the response of the X–M–X angle to the d-electron count of M in the case of X = SPh as compared to X = halides was also in question.

Unfortunately, the green complex 3, synthesized first by Green and Douglas in 1972 according to eq 1,[6] is quite

$$\underset{1}{Cp_2Nb(SPh)_2} \xrightarrow[\text{toluene}]{(C_7H_8)Mo(CO)_4} \underset{3}{Cp_2Nb(\mu\text{-}SPh)_2Mo(CO)_4} \quad (1)$$

insoluble in most organic solvents, a characteristic that has prevented development of its chemistry, as well as procurement of crystals suitable for X-ray crystallographic analysis. Since it was known that 1 could be easily oxidized upon reaction with iodine (eq 2), attempts to oxidize the

$$\underset{1}{Cp_2Nb(SPh)_2} \xrightarrow{I_2} \underset{2}{[Cp_2Nb(SPh)_2]I} \quad (2)$$

$$\underset{3}{Cp_2Nb(\mu\text{-}SPh)_2Mo(CO)_4} \xrightarrow[EtOH]{[NO][PF_6]} \underset{4}{[Cp_2Nb(\mu\text{-}SPh)_2Mo(CO)_4]PF_6} \quad (3)$$

neutral heterobimetallic by one-electron oxidants such as $[NO][PF_6]$ or $[Cp_2Fe][PF_6]$ were also successful, yielding the cationic species $Cp_2Nb(\mu\text{-}SPh)_2Mo(CO)_4^+$ (4) nicely crystalline as its PF_6^- salt (eq 3). Similarly, $[NO][PF_6]$ is a suitable oxidant for 1, yielding the crystalline salt of 2, $[Cp_2Nb(SPh)_2][PF_6]$. This report is of the X-ray crystal structures of 1, 2, and 4. Electrochemical properties of these complexes as well as variable-temperature NMR studies of 4 are also reported herein.

Experimental Section

Methods and Materials. An argon-filled drybox or Schlenk line techniques were used for the manipulations and transfer of

† On leave of absence from the Chemical Crystallography Laboratory at the University of Oxford, Oxford, England.

(1) Hoffman, R.; Lauher, J. W. *J. Am. Chem. Soc.* **1976**, *98*(7), 1729.
(2) (a) Alcock, N. W. *J. Chem. Soc. A* **1967**, 2001. (b) Petersen, J. L.; Dahl, L. F. *J. Am. Chem. Soc.* **1975**, *97*, 6416.
(3) (a) Prout, K.; Cameron, T. S.; Forder, R. A.; Critchley, S. R.; Denton, B.; Rees, G. V. *Acta Crystallogr., Sect. B* **1974**, *30*, 2290. (b) Green, J. C.; Green, M. L. H.; Prout, C. K. *J. Chem. Soc., Chem. Commun.* **1972**, 421. (c) Prout, K.; Critchley, S. R.; Rees, G. V. *Acta Crystallogr., Sect. B* **1974**, *30*, 2305. (d) Green, M. L. H. *Pure Appl. Chem.* **1972**, *30*, 373. (e) Petersen, J. L.; Dahl, L. F. *J. Am. Chem. Soc.* **1975**, *97*, 6422.
(4) Muller, E. G.; Watkins, S. F.; Dahl, L. F. *J. Organomet. Chem.* **1976**, *111*, 73.
(5) Dahl, L. F.; Petersen, J. L.; Lichtenberger, D. L.; Fenske, R. F. *J. Am. Chem. Soc.* **1975**, *97*, 6433.
(6) Green, M. L.; Douglas, W. E. *J. Chem. Soc., Dalton Trans.* **1972**, 1796.

0276-7333/89/2308-1315$01.50/0

samples. Nitrogen was predried over an in-line column consisting of molecular sieves, calcium chloride and calcium sulfate. Tetrahydrofuran (THF) and toluene were distilled under nitrogen from sodium/benzophenone. Methanol and ethanol were distilled from MgI_2. Heptane, spectrometric grade, was left over molecular sieves, and nitrogen was purged through it. Acetone was dried over barium oxide and stored over 3A molecular sieves, under nitrogen. All solvents were used immediately following distillation or stored under nitrogen over the appropriate molecular sieves. Cp_2NbCl_2 and other reagents were used as received from standard vendors, without further purification. The KSPh was prepared by reacting KH with PhSH in THF. (*Caution*: H_2 evolves; vent well.) The resulting white precipitate was filtered, washed with THF, and dried in vacuo. Infrared spectra were recorded in an IBM FTIR/32 or IBM FTIR/85 spectrometer. Nuclear magnetic resonance spectra were performed by using the Varian spectrometers XL 200, XL 400, and XL 200E. Electron-impact mass spectra were recorded on a VG Analytical 70-S mass spectrometer. Fast atom bombardment mass spectra were also recorded on the same instrument using neutral argon as the bombarding gas at 6–8 keV energy, in a matrix of *m*-nitrobenzyl alcohol. ESR spectra were recorded on a Varian E-6S spectrometer. Electronic spectra were taken on an IBM 9420 vis–UV spectrometer.

A Bioanalytical Systems 100A voltammograph was used for cyclic voltammetry studies. The potentials were referred to a $Ag^0/AgCl$ electrode with Pt^0 metal as the working electrode. The auxiliary electrode was Pt^0 wire. Solutions were 1 mM in solute and 0.1 M in supporting electrolyte $[Bu_4N][PF_6]$. The niobium samples and the supporting electrolyte were weighed inside the glovebox. Purified solvents were syringed into the cell containing the supporting electrolyte under a flow of N_2 at the electrochemical instrument bench.

Elemental analyses were performed by Galbraith Laboratories, Knoxville, TN.

Syntheses. $Cp_2Nb(SPh)_2$ (1). The preparation of this compound is a modification of the process of Green and Douglas.[6] In a 100-mL Schlenk flask were added 0.500 g (1.70 mmol) of Cp_2NbCl_2 and 0.557 g (3.06 mmol) of KSPh in 20 mL of ethanol. A color change from brown to violet occurred immediately after the addition of the solvent. After being refluxed for 2 h, the solution was cooled to room temperature, and the solvent was removed under vacuum. The residue was extracted with toluene and filtered. The volume of toluene was reduced and, upon addition of heptane, a green microcrystalline solid precipitated. MS: m/z = 441 ($M^+ = (C_5H_5)_2Nb(SC_6H_5)_2^+$); 332 ($M^+$ – SPh); 223 (M^+ – 2 SPh). Vis–UV: 465 and 540 nm.

$[Cp_2Nb(SPh)_2][PF_6]$ (2). Into a 100-mL Schlenk flask was loaded 100 mg (0.226 mmol) of $Cp_2Nb(SPh)_2$, 0.0435 g (0.2486 mmol) of $[NO][PF_6]$, and 10 mL of THF. Upon reaction with $[NO][PF_6]$ the red-brown solution of $Cp_2Nb(SPh)_2$ turns immediately to violet. The solvent was removed under vacuum, and the residue was extracted with acetone. Upon addition of heptane, a violet microcrystalline precipitate was obtained. ^1H NMR (δ, acetone-d_6): 6.66 (s, 10 H, $2C_5H_5$); 7.4–7.6 (m, 10 H, $2C_6H_5$). Anal. Calcd for $[Cp_2Nb(SPh)_2][PF_6]$ (Found): C, 45.06 (48.61); H, 3.44 (3.44).

$Cp_2Nb(\mu\text{-}SPh)_2Mo(CO)_4$ (3). A simple modification of the procedure used by Green and Douglas for the μ-SMe derivative yielded a green precipitate, insoluble in all normal solvents, as reported.[6] IR (KBr pellet): ν(CO) 2053 (w), 2013 (m), 1904 (vs), 1875 (m), 1855 (s), 1850 (m, sh), 1827 (s) cm^{-1}. These seven bands were assumed to be due to a mixture of $Cp_2Nb(\mu\text{-}SPh)_2Mo(CO)_4$ and $Cp_2Nb(SPh)(\mu\text{-}SPh)Mo(CO)_5$, as described in Results and Discussion.

$[Cp_2Nb(\mu\text{-}SPh)_2Mo(CO)_4][PF_6]$·Acetone (4). Into a 100-mL Schlenk flask were added 300 mg (0.462 mmol) of $Cp_2Nb(\mu\text{-}SPh)_2Mo(CO)_4$, prepared and isolated according to Green and Douglas' procedure,[6] and 0.0889 mg (0.508 mmol) of $[NO][PF_6]$, in 20 mL of ethanol, with stirring. Immediately after the addition of the solvent a brown solid precipitated and the evolution of a yellowish brown gas was observed. After the starting material was completely consumed, becoming solubilized upon reaction, the solvent was removed in vacuo and the residue was extracted with acetone. The volume of acetone was reduced, and, upon addition of heptane, brown crystals precipitated. These were filtered, washed with heptane, and dried under vacuum. The yield was 72%. Anal. Calcd for $[Cp_2Nb(\mu\text{-}SPh)_2Mo(CO)_4][PF_6]$·acetone (Found): C, 39.43 (39.21); H, 3.05 (3.40); S, 7.51 (7.73). ^1H NMR (δ, CD_3CN at 22 °C): 2.06 (s, 6 H, $2CH_3$); 7.84–7.50 (m, 10 H, $2C_6H_5$); 6.42–5.4 (br, 10 H, C_5H_5). See variable-temperature ^1H NMR studies below. Infrared (in acetone): ν(CO) 2056 (s), 1999 (shoulder), 1988 (m), 1945 (s) cm^{-1}. ^{13}C NMR (ppm, acetone-d_6, at 22 °C): 109.9 (br, C_5H_5); {130.3; 130.9; 132.5, 139.8 (C_6H_5)}; 205.9 (*C*O); 213.42 (*C*O). Vis–UV: 560.8 and 465.2 nm. FAB, mass spectrum: m/z = 651 ($M^+ = (C_5H_5)_2Nb(SC_6H_5)_2Mo(CO)_4^+$); 623 ($M^+$ – CO); 595 (M^+ – 2 CO); 567 (M^+ – 3 CO); 539 (M^+ – 4 CO); 461 (M^+ – (4CO + C_6H_6)); 443 (M^+ – $Mo(CO)_4$).

$Mo(CO)_4$(norbornadiene). This compound was prepared according to the literature procedure.[7]

X-ray Crystal Structure Determination

$Cp_2Nb(SPh)_2$. Details of the crystallographic data collection and refinement for compounds **1**, **2**, and **4** are summarized in Table I. The crystal mounting technique and data collection were identical for all compounds and are described below in detail only for **1**.

A green platelike crystal (0.01 mm × 0.20 mm × 0.41 mm) was mounted in mineral oil, on a glass fiber, in a random orientation at room temperature and quickly cooled to −100 °C in an N_2 cold stream. Preliminary examination and data collection were performed on a Nicolet R3m/V diffractometer.[8] Mo Kα (λ = 0.71073 Å) radiation, operating at 1500 W, and an oriented graphite crystal monochromator were used in all experiments. Cell constants were obtained from the refinement of 25 reflections ($2\theta_{av}$ = 19.54°). Omega scans of several intense reflections revealed slightly broadened peaks (~0.5° at half height) which indicated poor crystal quality. Several crystals were examined. Each crystal reflected the effect. Finally the best crystal of those examined was chosen for data collection. Examination of the cell parameters suggested an orthorhombic system. Axial photographs verified the Laue group assignment of *mmm*. Systematic absences indicated that the space group was *Pbca*. The data were collected at −100 (1) °C employing θ–2θ scanning techniques with a variable scan rate (2.03–29.30 deg/min). The scan range was 1.20° plus the Kα separation. The diameter of the collimated X-ray beam was 1.0 mm. A total of 6823 reflections were collected of which 211 were standards (three standards were collected every 97

Table I. Summary of Crystallographic Data for $Cp_2Nb(SPh)_2$ (1), $[Cp_2Nb(SPh)_2][PF_6]$ (2), and $[Cp_2Nb(\mu\text{-}SPh)_2Mo(CO)_4][PF_6]$·Acetone (4)

	1	2	4
mol formula	$C_{22}H_{20}S_2Nb$	$C_{22}H_{20}F_6PS_2Nb$	$C_{29}H_{26}O_5F_6PS_2NbMo$
fw	441.4	586.4	852.4
space group	*Pbca*	*C*2/*c*	*C*2/*c*
a, Å	13.756 (4)	12.058 (2)	33.85 (2)
b, Å	21.532 (6)	16.954 (4)	12.409 (4)
c, Å	25.601 (6)	11.079 (2)	15.708 (8)
β, deg		95.14 (1)	96.26 (4)
V, Å^3	7583 (3)	2256 (1)	6558 (5)
temp, °C	−100 (1)	−80 (1)	−100 (1)
Z	16	4	8
D(calcd), g cm^{-3}	1.547	1.727	1.727
radiatn	Mo Kα (λ = 0.710 73 Å)		
μ, cm^{-1}	8.21	8.15	9.47
index ranges	$-15 \le h \le 16$	$-14 \le h \le 14$	$-40 \le h \le 40$
	$-19 \le k \le 25$	$0 \le k \le 20$	$0 \le k \le 14$
	$-11 \le l \le 30$	$-13 \le l \le 0$	$0 \le l \le 18$
data to parameter ratio	19.0:1	12.5:1	8.5:1
R^a	0.0731	0.0445	0.0825
wR^a	0.0931	0.0652	0.0930
S^a	1.68	2.38	1.73
g	0.001 (fixed)	0.0004 (refined)	0.001 (fixed)

[a] $wR = [\sum w(F_o - F_c)^2/\sum w(F_o)^2]^{1/2}$. $w = [\sigma^2(F) + gF^2]^{-1}$. $S = [\sum w(F_o - F_c)^2/N_{data} - N_{par}]^{1/2}$.

(7) Bennett, M. A.; Pratt, L.; Wilkinson, G. *J. Chem. Soc.* **1961**, 2037.

(8) Software for diffractometer operation (P3VAX, V 3.1) was supplied by Nicolet Instrument Corp. Data reduction and absorption correction SHELXTL-PLUS (revision 3.4) was employed for structure solution, refinement, and graphics manipulation, G. M. Sheldrick 1988, supplied by Nicolet Instrument Corp.

reflections), and 2791 were flagged as observed, $|F| \geq 6\sigma|F|$. No significant change in the intensity of the standards was seen. Lorentz and polarization corrections were applied to the data. Data was smoothed by a learnt peak profiling technique.[9a] An empirical ellipsoid absorption correction[9b] was applied (μr = 0.11, ψ_{start} = 0.0°, ψ_{end} = 345.0°, $\Delta\psi$ = 15.0°, T_{min} = 0.755, T_{max} = 0.836, R_{int}[10] before 0.027 and after 0.023). The molecular structure was solved by direct methods[8] employing 6190 reflections. Niobium and sulfur were refined anisotropically, while all carbons were refined isotropically. Hydrogen atoms were placed in idealized positions, and their individual isotropic thermal motion was fixed at 0.08. The structure was refined to convergence by full-matrix least-squares methods[8] [quantity minimized $\sum w(F_o - F_c)^2$, where $w = (\sigma^2(F) + 0.001F^2)^{-1}$; at convergence the largest and mean Δ/σ = 0.415 and 0.009, respectively]. Largest peak in the final difference Fourier map was 1.09 e Å^{-3} while the smallest hole was −0.88 e Å^{-3}. Neutral atom scattering factors were taken from ref 11. The phenyl rings C1 to C6 and C7 to C12 were restrained to idealized hexagons (C–C bond length = 1.395 Å).[8] The Cp rings C51 to C55, C56 to C60, C61 to C65, and C66 to C70 were restrained to idealized pentagons (C–C bond length = 1.42 Å).[8]

$[Cp_2Nb(SPh)_2][PF_6]$. Cell constants for a violet platelike crystal (0.06 mm × 0.22 mm × 0.24 mm) were obtained from the refinement of 25 reflections ($2\theta_{av}$ = 21.24°). Omega scans of several intense reflections sharp peaks (~0.3 at half-height) indicated acceptable crystal quality. Examination of the cell parameters suggested a monoclinic system. Axial photographs verified the Laue group of $2/m$. Systematic absences indicated that the space group was $C2/c$. A total of 2180 reflections were collected of which 67 were standards (3 standards were collected every 97 reflections), and 1776 were flagged as observed, $|F| \geq 4\sigma|F|$. Lorentz and polarization corrections were applied to the data. Data was smoothed by a learnt peak profiling technique.[9a] An empirical ellipsoidal absorption correction[9b] was applied (μr = 0.10, ψ_{start} = 0.0°, ψ_{end} = 345.0°, $\Delta\psi$ = 15.0°, T_{min} = 0.687, T_{max} = 0.792, R_{int}[10] before 0.0282 and after 0.0215). The molecular structure was solved by direct methods.[8] All non-hydrogen atoms were refined anisotropically. Hydrogen atoms were placed in idealized positions, and their individual isotropic thermal motion was fixed at 0.08. The structure was refined to convergence by full-matrix least-squares methods[8] [quantity minimized $\sum w(F_o - F_c)^2$, where $w = (\sigma^2(F) + 0.0004F^2)^{-1}$; at convergence the largest and mean Δ/σ = 0.004 and 0.0001, respectively]. Largest peak in the final difference Fourier map was 1.12 e Å^{-3}, the smallest hole was −1.01 e Å^{-3}. Neutral atom scattering factors were taken from ref 11.

The PF_6 anion was found to lay about a twofold axis with the P atom occupying the special position $^1/_2$, y, $^1/_4$. The twofold axis was found to bisect two of the angles formed by the four meridial F atoms rendering only one-half of the molecule unique. To ensure an idealized octahedral coordination sphere for the P atom, the x coordinate of the two unique meridial F atoms (F(1) and F(2)) were fixed to the x coordinate of the P atom ($x = {}^1/_2$). Likewise the z coordinate of the two atoms were fixed to each other and allowed to refine as a single variable. The coordinates for the axial F atom (F(3)) was also constrained. In this case the z coordinate was fixed to the z coordinate of the P atom ($z = {}^1/_4$). The y coordinate was tied to the y coordinate of the P atom, and the two were refined as a single variable.

$[Cp_2Nb(\mu\text{-}SPh)_2Mo(CO)_4][PF_6]\cdot$Acetone. Cell constants for a brown platelike crystal (0.03 mm × 0.36 mm × 0.46 mm) were obtained from the refinement of 25 reflections ($2\theta_{av}$ = 20.20°). Omega scans of several intense reflections sharp peaks (~0.3° at half-height) indicated acceptable crystal quality. Examination of the cell parameters suggested a monoclinic system. Axial photographs verified the Laue group of $2/m$. Systematic absences indicated that the space group was $C2/c$. A total of 6315 reflections were collected of which 195 were standards (3 standards were collected every 97 reflections), and 3272 were flagged as observed, $|F| \geq 4\sigma|F|$. A significant decrease (30%) in intensity of the standard reflections was seen over the course of data collection. The data was corrected for the intensity decay by fitting the reflections to a smoothed intensity curve of the standard reflections. Lorentz and polarization corrections were applied to the data. Data was smoothed by a learnt peak profiling technique.[9a] An empirical ellipsoidal absorption correction[9b] was applied (μr = 0.24, ψ_{start} = 0.0°, ψ_{end} = 345.0°, $\Delta\psi$ = 15.0°, T_{min} = 0.702, T_{max} = 1.00, R_{int}[10] before 0.087 and after 0.071). The molecular structure was solved by direct methods[8] employing 6315 reflections. All atoms, except those for the occluded acetone molecule, were located in the resulting E map and were included for future anisotropic refinement. Hydrogen atoms were placed in idealized positions, and their individual isotropic thermal motion was fixed at 0.08. The structure was refined to convergence by full-matrix least-squares methods[8] [quantity minimized $\sum w(F_o - F_c)^2$, where $w = (\sigma^2(F) + 0.001F^2)^{-1}$; at convergence the largest and mean Δ/σ = 0.062 and 0.0001, respectively; largest peak in the final difference Fourier map was 0.99 e Å^{-3}; the smallest hole was −1.32 e Å^{-3}]. An occluded acetone molecule was located in a difference Fourier map near the final stages of refinement. The atoms of the acetone molecule were refined isotropically. Neutral atom scattering factors were taken from ref 11. The atomic distances in the acetone molecule were restrained with the routine DFIX, in the SHELXTL-PLUS program package, to idealized values.

Results and Discussion

Crystals of $Cp_2Nb(SPh)_2$ to be used for X-ray crystallographic analysis were obtained from toluene/heptane and crystals of $[Cp_2Nb(SPh)_2][PF_6]$ and $[Cp_2Nb(\mu\text{-}SPh)_2Mo(CO)_4][PF_6]$ grew at the solvent interface of hexane or heptane layered over acetone solutions of the salts. Compound **1** is green, paramagnetic and reactive to oxidants; the salts **2** and **4** are purple and brown, respectively, relatively air-stable, diamagnetic, and soluble in organic solvents such as acetone, THF, CH_3CN, and CH_2Cl_2. Whereas **4** is stable in THF and acetone, in CH_3CN decomposition occurs within 24 h, even in an inert atmosphere. The formulation of **4** was indicated by C, H, and S elemental analyses as well as its FAB mass spectrum which clearly showed the loss of four successive CO groups from the $[Cp_2Nb(SPh)_2Mo(CO)_4]^+$ parent ion.

X-ray Crystal Structures. X-ray crystal structure determinations of **1**, **2**, and **4** were carried out. Crystallographic data for all are summarized in Table I. Atom positions and selected bond length and bond angle parameters are presented for **1** in Tables II and III, respectively; for **2** in Tables IV and V, respectively; and for **4** in Tables VI and VII, respectively. The molecular structures and labeling schemes of **1**, **2**, and **4** are shown in Figures 1, 2, and 3a, respectively. Complete tables of bond lengths and angles, anisotropic thermal parameters, and hydrogen atom coordinates are given in supplementary material, as are packing diagrams for the three compounds.

As shown in Figure 1, the crystal structure of $Cp_2Nb(SPh)_2$ was determined to have two independent molecules per unit cell. The structural parameters of each individual $Cp_2Nb(SPh)_2$ molecule were substantially the same. They showed Nb–S–C_{Ph} angles of ca. 110°, indicating the tetrahedral disposition of the lone pairs of electrons on sulfur, and the latent potential of the $Cp_2Nb(SPh)_2$ unit to serve as a bidentate ligand, as it does in compounds **3** and **4**. The crystal packing diagram of **1** indicates an interesting relatively close approach (within 2.71 (1) Å) of a hydrogen on a Cp ring with the sulfur on an adjacent molecule.

The angle defined by the vectors connecting the centroids of the Cp rings to Nb is 132.4°. The S–Nb–S angle is 74.8 (1)° [S(1)–Nb(1)–S(2)] in one independent $Cp_2Nb(SPh)_2$ molecule and 76.1 (2)° [S(3)–Nb(2)–S(4)] in the other. This is smaller than any ∠X–M–X angle re-

(9) (a) Diamond, R. *Acta Crystallogr., Sect. A* **1969**, *25*, 43. (b) North, A. C. T.; Philips, D. C.; Matthews, F. S. *Acta Crystallogr., Sect. A* **1968**, *24*, 351.

(10) $R_{int} = [\sum(F_{mean} - F)^2/(n-1)\sum F^2]^{1/2}$.

(11) Gromer, D. T.; Waber, J. T. *International Tables for X-Ray Crystallgraphy*; The Kynoch Press: Birmingham, England, 1974; Vol. IV, pp 55, 99.

Table II. Atomic Coordinates (×10⁴) and Equivalent Isotropic Displacement Coefficients (Å² × 10³) for $Cp_2Nb(SPh)_2$ (1)

	x	y	z	U(eq)[a]
Nb(1)	5423 (1)	2351 (1)	5097 (1)	22 (1)
S(1)	6877 (3)	1652 (2)	5198 (2)	27 (1)
C(1)	5972 (6)	661 (4)	4680 (4)	31 (4)
C(2)	5983	85	4432	27 (4)
C(3)	6865	-213	4334	41 (5)
C(4)	7737	66	4485	33 (5)
C(5)	7726	642	4733	30 (4)
C(6)	6844	940	4830	26 (4)
S(2)	6696 (3)	3007 (2)	5542 (2)	32 (1)
C(7)	5973 (10)	3687 (5)	6352 (4)	47 (5)
C(8)	5551	4211	6578	61 (6)
C(9)	5256	4706	6264	64 (6)
C(10)	5384	4677	5724	67 (6)
C(11)	5806	4153	5498	44 (5)
C(12)	6101	3658	5812	36 (4)
C(51)	4458 (7)	2526 (6)	4331 (5)	31 (4)
C(52)	4946	3094	4436	44 (5)
C(53)	5958	2994	4365	49 (5)
C(54)	6095	2365	4217	40 (5)
C(55)	5168	2076	4195	53 (6)
C(56)	4329 (9)	2644 (4)	5806 (5)	31 (4)
C(57)	4955	2174	6001	39 (5)
C(59)	4763	1619	5720	34 (4)
C(58)	4018	1746	5352	33 (4)
C(60)	3749	2380	5405	38 (4)
Nb(2)	7514 (1)	1392 (1)	7378 (1)	22 (1)
S(3)	5995 (3)	945 (2)	6977 (2)	28 (1)
C(13)	6487 (9)	209 (4)	6137 (4)	36 (5)
C(14)	6664	-356	5888	39 (5)
C(15)	6616	-910	6170	41 (5)
C(16)	6392	-898	6701	55 (6)
C(17)	6216	-334	6951	36 (4)
C(18)	6263	220	6669	20 (4)
S(4)	6364 (3)	2294 (2)	7347 (2)	36 (1)
C(19)	6046 (6)	3366 (6)	7891 (5)	44 (5)
C(20)	6320	3882	8186	60 (6)
C(21)	7296	3978	8310	59 (6)
C(22)	7999	3557	8138	56 (6)
C(23)	7725	3042	7843	42 (5)
C(24)	6749	2946	7719	39 (5)
C(61)	7632 (10)	1599 (4)	8313 (5)	38 (4)
C(62)	6796	1224	8235	46 (5)
C(63)	7108	639	8041	58 (6)
C(64)	8137	652	8001	61 (6)
C(65)	8461	1246	8169	50 (6)
C(66)	9096 (9)	1161 (5)	7012 (5)	50 (5)
C(67)	8403	1002	6623	40 (5)
C(68)	7938	1556	6456	48 (5)
C(69)	8344	2059	6742	43 (5)
C(70)	9059	1815	7085	45 (5)

[a] Equivalent isotropic U defined as one-third of the trace of the orthogonalized U_{ij} tensor.

ported for a number of analogous d^1 structures: Cp_2NbCl_2, 85.6 (1)° (average);[3a] $Cp_2MoCl_2^+$, 82.0 (2)°;[3a] $(\eta^5\text{-}CH_3C_5H_4)_2VCl_2$, 87.1 (1)°;[3e] Cp_2VS_5, 89.3 (1)°;[12a] and $Cp_2V(SPh)_2$, 94.1 (1)°.[4] The interatomic S···S distance in $Cp_2Nb(SPh)_2$ is 3.058 (6) [S1···S2] and 3.098 (6) Å [S3···S4] for the two molecules in the unit cell. This is well beyond bonding interaction but considerably less than the S···S distance in analogous complexes.

As expected[1-5] the ∠S–Nb–S increases in the d^0, Nb(V) complex, $Cp_2Nb(SPh)_2^+$ (101.8 (1)° [S1–Nb–S1a]) as compared to the d^1, Nb(IV) (75 (1)° average) analogue. The magnitude of the increase, ca. 25°, is, however, unprecedented in analogous Cp_2MX_2 systems.[3a] For example whereas the ∠S–M–S is 99.3 (3)° for the d^0 Ti(IV) complex $Cp_2Ti(SPh)_2$, the angle decreases by only 5° in the d^1 $Cp_2V(SPh)_2$ analogue (∠S–V–S = 94.1 (1)°).[4] Neither is the small angle a heavier metal effect as is seen for the two complexes referenced above, Cp_2NbCl_2 and $(\eta^5\text{-}CH_3C_5H_4)_2VCl_2$.

(12) Muller, E. G.; Petersen, J. L.; Dahl, L. F. *J. Organomet. Chem.* **1976**, *111*, 91.

Table III. Selected Bond Lengths (Å) and Angles (deg) for $Cp_2Nb(SPh)_2$ (1)

Bond Lengths			
Nb(1)–S(1)	2.516 (5)	Nb(1)–S(2)	2.522 (5)
Nb(1)–C(51)	2.398 (12)	Nb(1)–C(52)	2.419 (12)
Nb(1)–C(53)	2.442 (12)	Nb(1)–C(54)	2.436 (12)
Nb(1)–C(55)	2.409 (13)	Nb(1)–C(56)	2.442 (12)
Nb(1)–C(57)	2.434 (12)	Nb(1)–C(59)	2.420 (11)
Nb(1)–C(58)	2.421 (12)	Nb(1)–C(60)	2.434 (13)
S(1)–C(6)	1.799 (11)	S(2)–C(12)	1.763 (12)
Nb(2)–S(3)	2.518 (5)	Nb(2)–S(4)	2.506 (5)
Nb(2)–C(61)	2.443 (12)	Nb(2)–C(62)	2.433 (13)
Nb(2)–C(63)	2.415 (11)	Nb(2)–C(64)	2.412 (11)
Nb(2)–C(65)	2.430 (13)	Nb(2)–C(66)	2.420 (13)
Nb(2)–C(67)	2.435 (13)	Nb(2)–C(68)	2.454 (13)
Nb(2)–C(69)	2.451 (12)	Nb(2)–C(70)	2.430 (13)
S(3)–C(18)	1.788 (10)	S(4)–C(24)	1.777 (13)
Bond Angles			
S(1)–Nb(1)–S(2)	74.8 (1)	Nb(1)–S(1)–C(6)	115.8 (3)
S(1)–C(6)–C(5)	117.6 (3)	Nb(1)–S(2)–C(12)	107.5 (5)
S(2)–C(12)–C(7)	118.9 (4)	S(2)–C(12)–C(11)	121.0 (4)
S(3)–Nb(2)–S(4)	76.1 (2)	Nb(2)–S(3)–C(18)	110.1 (4)
S(3)–C(18)–C(13)	119.4 (3)	S(3)–C(18)–C(17)	120.5 (3)
Nb(2)–S(4)–C(24)	114.0 (4)	S(4)–C(24)–C(19)	118.3 (3)
S(4)–C(24)–C(23)	121.7 (3)		

Table IV. Atomic Coordinates (×10⁴) and Equivalent Isotropic Displacement Coefficients (Å² × 10³) for $[Cp_2Nb(SPh)_2][PF_6]$ (2)

	x	y	z	U(eq)[a]
Nb	0	2693 (1)	2500	23 (1)
C(1)	-1942 (4)	2570 (3)	2875 (6)	42 (2)
C(2)	-1884 (4)	3128 (3)	1938 (5)	42 (2)
C(3)	-1288 (4)	3783 (3)	2414 (5)	39 (2)
C(4)	-958 (4)	3632 (3)	3643 (5)	37 (2)
C(5)	-1394 (4)	2895 (3)	3933 (5)	38 (2)
S(1)	-718 (1)	1790 (1)	931 (1)	29 (1)
C(6)	487 (4)	1273 (3)	-896 (4)	34 (1)
C(7)	1234 (4)	788 (3)	-1397 (5)	36 (2)
C(8)	1877 (4)	262 (3)	-690 (5)	42 (2)
C(9)	1765 (5)	233 (3)	548 (5)	44 (2)
C(10)	1013 (4)	711 (3)	1057 (5)	36 (2)
C(11)	363 (4)	1231 (3)	338 (4)	28 (1)
P	5000	1125 (1)	2500	55 (1)
F(1)	5000	458 (3)	1511 (4)	127 (3)
F(2)	5000	1754 (3)	1511 (4)	243 (7)
F(3)	3802 (6)	1125 (1)	2357 (12)	295 (8)

[a] Equivalent isotropic U defined as one-third of the trace of the orthogonalized U_{ij} tensor.

Table V. Selected Bond Lengths (Å) and Angles (deg) for $[Cp_2Nb(SPh)_2][PF_5]$ (2)

Bond Lengths			
Nb–C(1)	2.423 (5)	Nb–C(2)	2.416 (5)
Nb–C(3)	2.410 (5)	Nb–C(4)	2.395 (5)
Nb–C(5)	2.437 (5)	Nb–S(1)	2.417 (1)
Nb–C(1A)	2.423 (5)	Nb–C(2A)	2.416 (5)
Nb–C(3A)	2.410 (5)	Nb–C(4A)	2.395 (5)
Nb–C(5A)	2.437 (5)	Nb–S(1A)	2.417 (1)
C(1)–C(2)	1.412 (8)	C(1)–C(5)	1.406 (8)
C(2)–C(3)	1.399 (7)	C(3)–C(4)	1.407 (7)
C(4)–C(5)	1.403 (7)	S(1)–C(11)	1.783 (5)
C(6)–C(7)	1.373 (7)	C(6)–C(11)	1.391 (6)
C(7)–C(8)	1.378 (7)	C(8)–C(9)	1.391 (8)
C(9)–C(10)	1.374 (8)	C(10)–C(11)	1.383 (7)
P–F(1)	1.574 (5)	P–F(2)	1.529 (5)
P–F(3)	1.438 (7)	P–F(1A)	1.574 (5)
P–F(2A)	1.529 (5)	P–F(3A)	1.439 (7)
Bond Angles			
S(1)–Nb–S(1A)	101.4 (1)	Nb–S(1)–C(11)	112.0 (1)
S(1)–C(11)–C(6)	118.8 (3)	S(1)–C(11)–C(10)	121.4 (4)

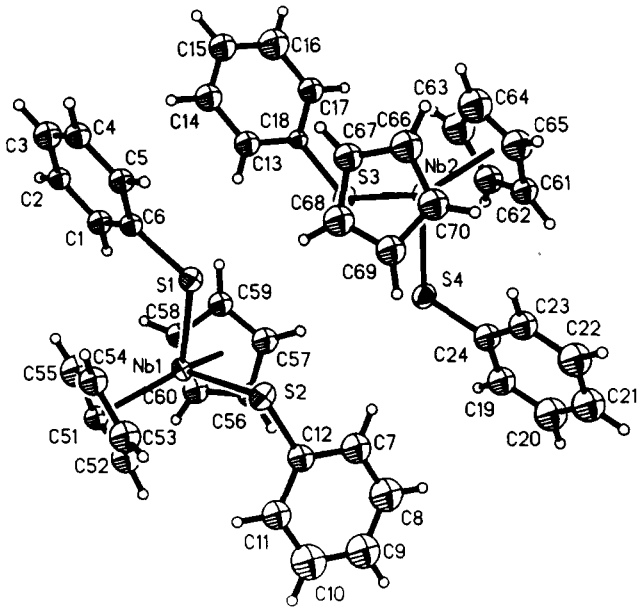

Figure 1. Thermal ellipsoid plot (50% probability) of $Cp_2Nb(SPh)_2$ (1) with complete numbering scheme for the two independent molecules in the unit cell.

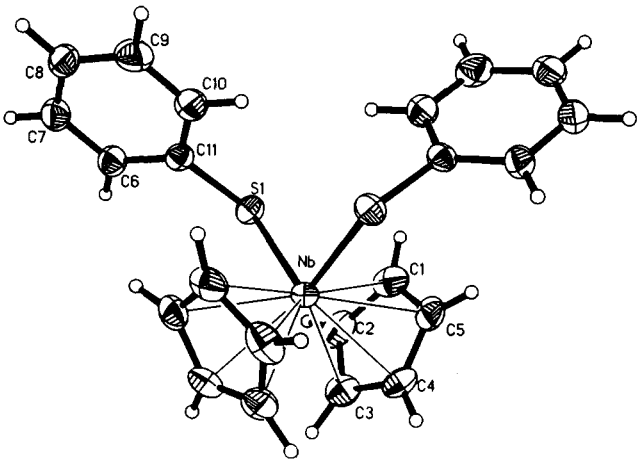

Figure 2. Thermal ellipsoid plot (50% probability) for the cation of $[Cp_2Nb(SPh)_2][PF_6]$ (2) with numbering scheme.

The major difference in the monomeric Nb(V) derivative $Cp_2Nb(SPh)_2^+$ and that unit in $Cp_2Nb(\mu\text{-}SPh)_2Mo(CO)_4^+$ was an increase of the Nb–S distances of an average of 2.417 (1) Å in **2** to ca. 2.499 (2) Å in **4**. The phenyl groups are almost identically arranged in the monomer and the heterobimetallic. The S–Nb–S angles are the same. The angle of the intersecting vectors from Nb to the centroid of the Cp rings is virtually the same in both compounds (128.5° in **2**; 132° in **4**). The coordination geometry about Mo in **4** is a relatively regular octahedron, however, with an obtuse S–Mo–S angle of 103.1 (1)°. The Mo–C–O units are acceptably linear, and the C–Mo–C angles are little distorted from 90°. As best seen in the view of **4** presented in Figure 3b, the $Nb(\mu\text{-}S)_2Mo$ core is planar. The Nb–S [2.499 (2) Å average] and Mo–S [2.476 (7) Å average] distances are about the same. The Nb–Mo distance of 3.116 (2) Å is known with good accuracy, and it is shorter than the sum of the covalent radii of Nb and Mo (3.24 Å), but a bit longer than the direct Nb–Mo bond of Cp_2Nb–$Mo(CO)_3Cp$ (3.073 (1) Å).[13] The interatomic S···S distance

(13) Pasynskii, A. A.; Skripkin, Yu. V.; Eremenko, V. T.; Kalinnikov, V. T.; Aleksandrov, G. G.; Andrianov, V. G.; Struchkov, Yu. T. *J. Organomet. Chem.* **1979**, *165*, 46.

Table VI. Atomic Coordinates (×10⁴) and Equivalent Isotropic Displacement Parameters (Å² × 10³) for $[Cp_2Nb(\mu\text{-}SPh)_2Mo(CO)_4][PF_6]$•Acetone (4•Acetone)

	x	*y*	*z*	*U*(eq)[a]
Nb	3488 (1)	705 (1)	-31 (1)	47 (1)
Mo	4138 (1)	1747 (1)	1269 (1)	53 (1)
S(1)	3792 (1)	7 (3)	1381 (2)	57 (1)
S(2)	3836 (1)	2471 (3)	-126 (2)	54 (1)
C(1)	3905 (5)	-2146 (13)	1558 (12)	81 (7)
C(2)	4104 (5)	-3098 (5)	1714 (13)	88 (8)
C(3)	4512 (6)	-3051 (16)	1655 (13)	99 (9)
C(4)	4705 (5)	-2170 (16)	1504 (13)	94 (8)
C(5)	4494 (5)	-1206 (15)	1413 (10)	78 (7)
C(6)	4085 (4)	-1184 (13)	1442 (9)	64 (6)
C(7)	3507 (4)	4235 (12)	633 (11)	67 (6)
C(8)	3309 (5)	5238 (15)	571 (13)	92 (8)
C(9)	3143 (5)	5593 (16)	-186 (15)	96 (9)
C(10)	3196 (5)	5072 (14)	-947 (14)	91 (8)
C(11)	3394 (5)	4078 (13)	-906 (11)	74 (7)
C(12)	3554 (4)	3683 (11)	-104 (11)	61 (6)
C(13)	4413 (5)	3217 (17)	1387 (12)	88 (8)
O(13)	4585 (5)	3977 (13)	1470 (12)	152 (8)
C(14)	4463 (4)	1249 (15)	2342 (10)	73 (6)
O(14)	4641 (3)	1002 (13)	2972 (8)	116 (6)
C(15)	4580 (5)	1299 (12)	567 (10)	64 (6)
O(15)	4842 (3)	1149 (10)	185 (8)	92 (5)
C(16)	3721 (5)	2273 (13)	2037 (11)	70 (6)
O(16)	3530 (4)	2555 (10)	2549 (8)	99 (6)
C(17)	4000 (5)	-369 (14)	-584 (10)	73 (7)
C(18)	3656 (6)	-994 (13)	-611 (12)	85 (8)
C(19)	3366 (5)	-554 (18)	-1166 (12)	91 (8)
C(20)	3545 (5)	388 (15)	-1546 (9)	70 (7)
C(21)	3930 (6)	466 (12)	-1147 (10)	73 (7)
C(22)	2953 (4)	713 (16)	873 (11)	79 (7)
C(23)	3004 (4)	1759 (15)	608 (11)	71 (7)
C(24)	2900 (4)	1793 (13)	-277 (10)	61 (6)
C(25)	2797 (4)	776 (14)	-524 (11)	75 (7)
C(26)	2832 (4)	80 (15)	144 (13)	80 (7)
P	2348 (1)	2442 (3)	3004 (3)	65 (2)
F(1)	2303 (5)	3673 (10)	2907 (11)	185 (9)
F(2)	1927 (3)	2270 (15)	2592 (10)	208 (9)
F(3)	2156 (5)	2612 (12)	3865 (9)	169 (8)
F(4)	2393 (5)	1236 (10)	3137 (11)	172 (8)
F(5)	2763 (4)	2599 (12)	3477 (12)	187 (8)
F(6)	2510 (5)	2280 (14)	2167 (9)	191 (9)
O(1)	806 (10)	509 (23)	7037 (14)	350 (18)
C(50)	637 (10)	526 (19)	6304 (14)	232 (16)
C(51)	681 (9)	1426 (17)	5743 (16)	228 (15)
C(52)	463 (8)	1440 (17)	5918 (17)	229 (16)

[a] Equivalent isotropic *U* defined as one third of the trace of the orthogonalized U_{ij} tensor.

increases from 3.08 (3) Å in the neutral monomer to 3.742 (2) Å in **2** and to 3.882 (6) Å in **4**. The phenyl substituents on S are in the anti configuration (Figure 3) whereas in THF and acetone solution there is a nearly equal distribution of anti and syn conformers (vide infra). The crystal packing diagram for **4**•acetone (Figure 3S) shows an acetone solvent molecule within contact distance of a carbonyl oxygen atom; however, it does not appear to influence the geometry of the cation.

In Table VIII are listed two compounds of formula $Cp_2M(\mu\text{-}SR)_2Mo(CO)_4$ for comparison of their structural parameters with **4**. The $Cp_2Ti(\mu\text{-}SMe)_2Mo(CO)_4$ compound is isoelectronic with **4** and also contains acute ∠M–S–M′ and obtuse ∠S–M–S or ∠S–M′–S.[14] The $Cp_2W(\mu\text{-}SPh)_2Mo(CO)_4$ compound, judged *not* to contain a metal–metal′ bond,[15] has as expected a much greater M–Mo distance and a reversal of the bond angles; i.e., ∠M–S–M′ is obtuse and ∠S–M–S, acute.

^{1}H NMR Studies. The d^0, Nb(V) complex ion $Cp_2Nb(SPh)_2^+$ (as its PF_6^- salt in acetone-d_6 solution) has

(14) Davies, G. R.; Kilbourn, B. T. *J. Chem. Soc. A* **1971**, 87.
(15) Prout, K.; Rees, G. V. *Acta Crystallogr.* **1974**, *B30*, 2717.

Table VII. Bond Lengths (Å) and Angles (deg) for $[Cp_2Nb(\mu\text{-}SPh)_2Mo(CO)_4][PF_6]\cdot$Acetone (4·Acetone)

	Bond Lengths		
Nb-Mo	3.116 (2)	Nb-S(1)	2.498 (4)
Nb-S(2)	2.501 (4)	Nb-C(17)	2.422 (17)
Nb-C(18)	2.391 (17)	Nb-C(19)	2.371 (21)
Nb-C(20)	2.439 (15)	Nb-C(21)	2.444 (18)
Nb-C(22)	2.419 (17)	Nb-C(23)	2.399 (16)
Nb-C(24)	2.401 (13)	Nb-C(25)	2.381 (15)
Nb-C(26)	2.394 (15)	Mo-S(1)	2.471 (4)
Mo-S(2)	2.482 (4)	Mo-C(13)	2.048 (20)
Mo-C(14)	2.006 (15)	Mo-C(15)	2.031 (16)
Mo-C(16)	2.060 (17)	S(1)-C(6)	1.777 (16)
S(2)-C(12)	1.783 (14)	C(1)-C(2)	1.368 (23)
C(1)-C(6)	1.361 (22)	C(2)-C(3)	1.396 (27)
C(3)-C(4)	1.308 (28)	C(4)-C(5)	1.391 (26)
C(5)-C(6)	1.391 (21)	C(7)-C(8)	1.411 (24)
C(7)-C(12)	1.370 (23)	C(8)-C(9)	1.334 (29)
C(9)-C(10)	1.388 (31)	C(10)-C(11)	1.401 (23)
C(11)-C(12)	1.404 (22)	C(13)-O(13)	1.108 (26)
C(14)-O(14)	1.144 (19)	C(15)-O(15)	1.139 (20)
C(16)-O(16)	1.141 (22)	C(17)-C(18)	1.395 (25)
C(17)-C(21)	1.366 (22)	C(18)-C(19)	1.355 (26)
C(19)-C(20)	1.472 (28)	C(20)-C(21)	1.388 (25)
C(22)-C(23)	1.379 (27)	C(22)-C(26)	1.412 (26)
C(23)-C(24)	1.397 (23)	C(24)-C(25)	1.355 (23)
C(25)-C(26)	1.354 (26)	P-F(1)	1.541 (13)
P-F(2)	1.513 (13)	P-F(3)	1.577 (16)
P-F(4)	1.516 (13)	P-F(5)	1.528 (13)
P-F(6)	1.492 (16)	O(1)-C(50)	1.227 (33)
C(50)-C(51)	1.441 (33)	C(50)-C(52)	1.440 (33)
	Bond Angles		
Mo-Nb-S(1)	50.8 (1)	Mo-Nb-S(2)	51.0 (1)
S(1)-Nb-S(2)	101.8 (1)	Mo-Nb-C(17)	88.9 (4)
Nb-Mo-S(1)	51.5 (1)	Nb-Mo-S(2)	51.6 (1)
S(1)-Mo-S(2)	103.1 (1)	Nb-Mo-C(13)	135.3 (5)
S(1)-Mo-C(13)	170.5 (5)	S(2)-Mo-C(13)	84.1 (5)
Nb-Mo-C(14)	134.9 (5)	S(1)-Mo-C(14)	83.8 (5)
S(2)-Mo-C(14)	171.0 (5)	C(13)-Mo-C(14)	89.8 (7)
Nb-Mo-C(15)	92.3 (4)	S(1)-Mo-C(15)	100.5 (4)
S(2)-Mo-C(15)	82.9 (4)	C(13)-Mo-C(15)	86.4 (7)
C(14)-Mo-C(15)	90.2 (6)	Nb-Mo-C(16)	92.0 (4)
S(1)-Mo-C(16)	82.8 (5)	S(2)-Mo-C(16)	99.2 (5)
C(13)-Mo-C(16)	89.9 (7)	C(14)-Mo-C(16)	87.3 (6)
C(15)-Mo-C(16)	175.6 (6)	Nb-S(1)-Mo	77.7 (1)
Nb-S(1)-C(6)	120.7 (5)	Mo-S(1)-C(6)	117.7 (5)
Nb-S(2)-Mo	77.4 (1)	Nb-S(2)-C(12)	118.7 (5)
Mo-S(2)-C(12)	117.3 (6)	Mo-C(13)-O(13)	175.3 (18)
Mo-C(14)-O(14)	177.0 (16)	Mo-C(15)-O(15)	173.3 (13)
Mo-C(16)-O(16)	170.9 (14)		

a sharp resonance at 6.66 ppm assigned to the hydrogens on the Cp ring and a multiplet at 7.4–7.6 ppm assigned to the phenyl hydrogens. Narrow line widths indicate little if any relaxation broadening effects due to the quadrupolar nucleus of Nb.[16,17]

The proton magnetic resonances of 4 are temperature dependent. At 22 °C the ^1H NMR spectrum of 4·acetone in acetone-d_6 showed a multiplet in the phenyl region (7.84–7.50 ppm), a singlet for the acetone of crystallization at 2.06 ppm, and a broad peak in the Cp region was only barely discernible (Figure 4). When the temperature is raised to 40 °C, the Cp region sharpened somewhat into a broad peak centered around 5.8 ppm. When the temperature is lowered to 0 °C, the broad resonance resolved itself into three resonances with chemical shifts at 5.40, 5.84, and 6.43 ppm (see Figure 4) which became even sharper, without changing positions, upon further cooling. Integration of the resonances in the Cp region with the Ph region was 1:1 at all temperatures. Integration of the three

(16) Labinger, J. A. In *Comprehensive Organometallic Chemistry*; Wilkinson, G., Stone, F. G. A., Abel, E., Eds.; Pergamon Press: London, 1982; Chapter 25.
(17) Davison, A.; Ellis, J. E. *J. Organomet. Chem.* **1970**, *23*, C1.

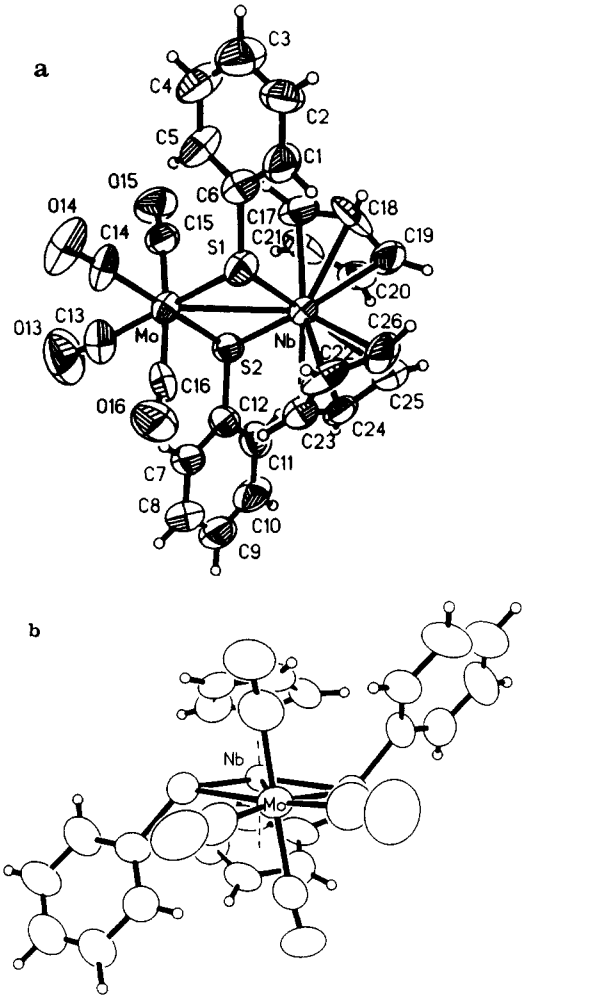

Figure 3. (a) Thermal ellipsoid plot (50% probability) for the cation of $[Cp_2Nb(\mu\text{-}SPh)_2Mo(CO)_4][PF_6]\cdot(CH_3)_2CO$ (4·acetone) with numbering scheme. (b) View of the cation of compound 4 along the Mo–Nb axis.

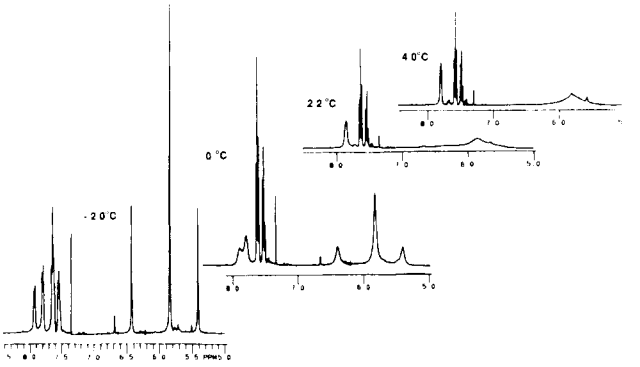

Figure 4. Variable-temperature ^1H NMR of $[Cp_2Nb(\mu\text{-}SPh)_2Mo(CO)_4][PF_6]\cdot$acetone, in acetone-$d_6$, at 400 MHz, at −20, 0, 22, and 40 °C.

resonances *within* the Cp region of the spectrum showed a distribution of 1:3:1 which was also invariant with temperature.

The variable-temperature NMR results are consistent with the presence of two isomeric forms of $Cp_2Nb(\mu\text{-}SPh)_2Mo(CO)_4^+$ in solution which interconvert on the NMR time scale at temperatures ≥0 °C. As suggested by structures A and B, the anti arrangement of SPh groups should yield the Cp groups chemically equivalent while the syn arrangement produces two different environments. Thus the resonances of equal intensity, at δ = 5.40 and 6.43

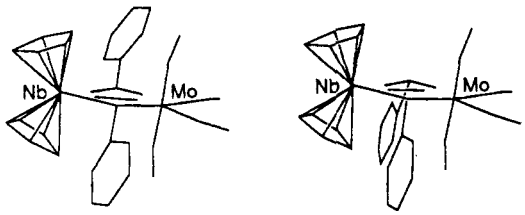

A B

ppm are assigned to the syn isomer and that at 5.84 ppm to the anti form. The relative proportion of anti to syn is 3:2; i.e., the anti form, the form that preferentially crystallizes out of acetone/heptane, only slightly predominates in solution. Structure A is a stick drawing of compound **4** according to molecular parameters taken from the X-ray structure, and B is modified to place the SPh groups in the syn configuration. In this model we left the Nb(μ-S_2)Mo core planar, as it is in **4** and also in $Cp_2Ti(\mu$-$SMe)_2Mo(CO)_4$.[14] The latter is, in fact, syn in the solid state; however, fluxionality is *also* seen for the $Cp_2Ti(\mu$-$SR)_2Mo(CO)_4$ compounds, interchanging syn and anti forms in solution.[18,24]

The most downfield resonances in the phenyl region of **4** also display temperature dependence. At +40 °C there is a doublet at 7.85 ppm, of relative ratio of 2:3 with respect to the rest of the multiplet in the phenyl region, indicating equivalence of all ortho protons in both isomeric forms of the $Cp_2Nb(\mu$-$SPh)_2Mo(CO)_4^+$ dimer. The coupling of 7.7 Hz is as expected for the meta- to ortho-hydrogen coupling. Upon cooling to 20 °C the resonance broadens, and at 0 °C two broad resonances separate out. By −20 °C these resonances are themselves resolved doublets with J = 7.44 Hz in each. The resonance at 7.92 ppm is 70% the integrated intensity of that one at 7.79 ppm. Thus, consistent with the isomeric ratio deduced from the interpretation of the cyclopentadienyl proton region, we ascribe the 7.92 ppm doublet to those ortho hydrogens on the phenyl rings of the syn isomeric form and the 7.79 ppm doublet to the anti form, structures B and A, respectively.

The ^{13}C NMR variable-temperature spectra are corroborative of the above interpretation. These spectra were measured on samples of **4** enriched in ^{13}C by allowing acetone solutions of **4** to stir under 1 atm of ^{13}CO overnight at room temperature. At 40 °C in acetone, there is one resonance for the Cp carbons at 110 ppm, which broadens and coalesces as the temperature is lowered. At temperatures of −20 °C and below the ^{13}C pattern is identical with the ^1H low-temperature spectra; i.e., three signals of relative ratio 1:3:1 at 110.7, 109.6, and 108.7 ppm, respectively, are observed.

Assuming the model of a 3:2 isomeric ratio of anti and syn isomers, one would predict the low-temperature limiting spectrum of the CO carbons to consist of five lines of relative intensity 3:3:1:1:2. In fact, at −60 °C five resonances in the CO region are observed, at 213.8, 212.9, 203.8, 201.4, and 198.1 ppm. Although relative intensities are to be interpreted with caution in ^{13}C NMR, the resonances at 203.8 and 198.1 ppm are clearly much less intense than the others and are assigned to the axial carbonyl carbons of the syn isomer. The two carbons trans to the sulfur ligands are expected to be the most deshielded. The resonances at 213.8 and 212.9 ppm are tentatively assigned to those trans carbonyls. As the temperature is increased, the carbonyl ^{13}C resonances broaden and coalesce (at 0 °C). We do not see the high-temperature limiting spectrum because the weighted average signal is hidden under that of the solvent, acetone.

In acetonitrile solvent the variable-temperature ^1H NMR is more complex. Upon warming above room-temperature, the broad Cp peak changes into two well-resolved resonances, and upon cooling there are more resonances than observed in the acetone solution spectra. Since CH_3CN is known to form adducts with niobium metallocenes[19] and in cases decompose them, the complexities are left unexplained.

ν(CO) Infrared Data. The observed seven-band spectrum of "$Cp_2Nb(\mu$-$SPh)_2Mo(CO)_4$" is interpreted as representing a mixture of a pentacarbonyl species, $Cp_2Nb(SPh)(\mu$-$SPh)Mo(CO)_5$ and the cis, disubstituted tetracarbonyl, **3**. Subtracting the bands at 2053 (w), 1904 (vs), and 1850 (m) cm^{-1} of pattern and position typical of C_{4v} species ($PhSMo(CO)_5^-$, for example, has bands at 2056 (w), 1921 (s), 1865 (m) cm^{-1})[20] leaves a four-band spectrum highly typical of a C_{2v} $M(CO)_4$ species. For two reasons then we cannot agree with the Green and Douglas interpretation that the seven-band spectrum observed for "$Cp_2Nb(\mu$-$SMe)_2Mo(CO)_4$" is indicative of a "symmetry lower than C_{2v}" for the $Mo(CO)_4$ unit and hence a syn arrangement of methyl groups with respect to the $Nb(S)_2$ Mo plane:[6] (1) the lowest symmetry possible, C_s, also predicts a four-band pattern for $Mo(CO)_4$ and (2) their observed spectrum is most assuredly that of a mixture of products, including $Mo(CO)_6$.

The ν(CO) IR of the $Mo(CO)_4$ moiety in the neutral and cationic dimers are now comparable and are listed below (KBr data) assuming C_{2v} symmetry. We can assign with confidence only the A_1^2 vibrational mode to the highest frequency band position.

	A_1^2	$A_1B_1B_2$
$Cp_2Nb(\mu$-$SPh)_2Mo(CO)_4$	2013 s	1875 s, 1855 s, 1827 s
$[Cp_2Nb(\mu$-$SPh)_2Mo(CO)_4]^+$	2058 s	1994 sh, 1986 s, 1945 s

Clearly the $Mo(CO)_4$ experiences the positive charge of the oxidized dimer as compared to the neutral analogue. We also conclude that within the available resolution the IR is sensitive only to the cis orientation of the donor sulfur atom and not to steric influences of the pendant Ph groups. That is, the presence of a mixture of anti and syn conformers, as evident from NMR results, is not distinguished by ν(CO)IR.

Electrochemical Studies. Cyclic voltammograms of compounds **1**, **2**, and **4** are shown in Figure 5. The general features of two reversible waves (or quasi reversible in the case of compound **4**) are observed for all. As seen in Figure 5B, the Nb(V) cationic monomer shows a redox wave at −0.29 V attributed to the reduction of Nb(V) to Nb(IV), and another at −1.15 V represents further reduction of Nb(IV) to Nb(III). As seen in Figure 5A, the Nb(IV) neutral monomer shows no cathodic current upon beginning the reduction scan at −0.3 V. A reversible wave is seen for Nb(IV) to Nb(III) reduction at −1.10 V and, upon return of the sweep, the oxidation at −0.28 V generates the Nb(V) species which is then reduced in the next cycle of the scan.

(18) Braterman, P. S.; Wilson, V. A.; Joshi, K. K. *J. Chem. Soc. A* **1971**, 191.
(19) Bunker, M. J.; DeCian, A.; Green, M. L. H.; Moreau, J. J. E.; Siganporia, N. *J. Chem. Soc., Dalton Trans.* **1980**, 2155.
(20) Darensbourg, D. J.; Sanchez, K.; Reibenspies, J. *Inorg. Chem.*, in press.
(21) Kotz, J. C.; Vinning, W.; Coco, W.; Rosen, R.; Dias, A. R.; Garcia, M. H. *Organometallics* **1983**, *2*, 68.
(22) Herrman, W. A.; Biersack, H.; Ziegler, M. L.; Balbach, B. *J. Organomet. Chem.* **1981**, *206*, C33.
(23) Köpf, H.; Räthlein, K. H. *Angew. Chem., Int. Ed. Engl.* **1969**, *8*(12), 980.
(24) Ruffing, C. J.; Rauchfuss, T. B. *Organometallics* **1985**, *4*, 524.

Table VIII. Bond Distances (Å) and Angles (deg) of Heterobimetallic Compounds of the Type $Cp_2M(SR)_2Mo(CO)_4$

compd	M···Mo	M–SR	Mo–SR	∠M–S–Mo	∠SMS	∠SMoS	ref
M = Ti	3.321 (2)	S_1, 2.475 (4)	S_1, 2.567 (4)	S_1, 82.4 (1)	99.9 (1)	94.6 (1)	14
R = CH_3		S_2, 2.445 (4)	S_2, 2.557 (4)	S_2, 83.2 (1)			
M = Nb	3.116 (2)	S_1, 2.498 (4)	S_1, 2.471 (4)	S_1, 77.7 (1)	101.8 (1)	103.1 (1)	this work
R = Ph		S_2, 2.501 (4)	S_2, 2.482 (4)	S_2, 77.4 (1)			
M = W	4.062 (3)	S_1, 2.526 (5)	S_1, 2.606 (6)	S_1, 104.6 (2)	72.6 (2)	69.1 (2)	15
R = Rh		S_2, 2.483 (6)	S_2, 2.621 (6)	S_2, 105.4 (2)			

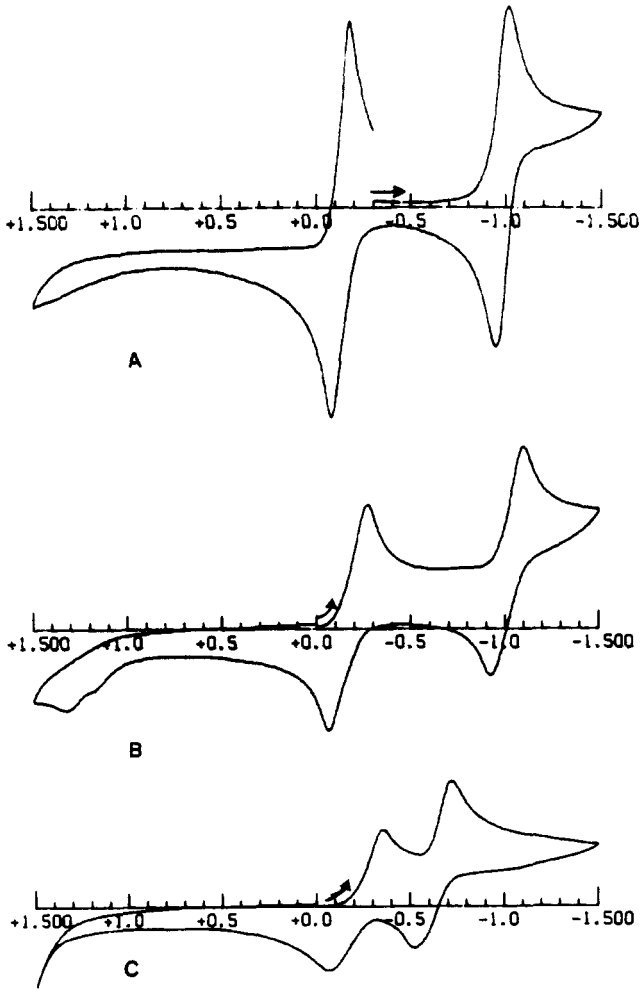

Figure 5. (A) Cyclic voltammogram of $Cp_2Nb(SPh)_2$, 1 mM in THF, containing 0.1 M $[Bu_4N][PF_6]$. Sweep rate was 200 mV/s. (B) Cyclic voltammogram of $[Cp_2Nb(SPh)_2][PF_6]$, 1 mM in acetone, containing 0.1 M $[Bu_4N][PF_6]$. Sweep rate was 200 mV/s. (C) Cyclic voltammogram of $[Cp_2Nb(\mu\text{-}SPh)_2Mo(CO)_4][PF_6]$·acetone, 1 mM in THF, containing 0.1 M $[Bu_4N][PF_6]$. Sweep rate was 200 mV/s.

The heterobimetallic cation **4** shows reduction waves at $E_{1/2}$ = –0.32 and –0.70 V (Figure 5C). Whereas the position of the first reduction is, within experimental error, the same as observed for the monomers, the second occurs at a considerably lower potential. In contrast to reports of $Cp_2Ti(\mu\text{-}SPh)_2M(CO)_4$ (M = Cr, Mo, W) in which an oxidation of the group 6 metal is suggested to occur at more positive potentials (at +0.6 V for M = W, for example),[21] we observed no redox wave to be associated with Mo in compound **4**.

The solvents used in the above electrochemical studies, THF and acetone, were selected for their solubilizing characteristics as well as for the stability of the compounds. In general the potentials recorded in both solvents were the same. However, in acetone compound **4** showed another reduction wave of low intensity at –1.1 V due to dimer disruption producing $Cp_2Nb(SPh)_2^+$. In fact, the instability of analogous complexes[19] in polar solvents such as acetonitrile is well-known and can yield extremely complicated mixed-ligand systems.

The irreversible oxidation producing a low intensity wave at +1.1 V for $Cp_2Nb(SPh)_2^+$ (Figure 5B) has been seen by other workers for an analogous system, Cp_2MoX_2 (X = halides or SR^-).[21] They accommodated this result by an ECE mechanism in which the intervening chemical event (after M(IV) → M(V) oxidation) involved reductive elimination of an SR· radical either in a solvent-assisted mononuclear manner or via a binuclear X-bridged complex, generating a new M(IV) species susceptible to further oxidation. The latter, binuclear path is particularly appealing for niobium compounds well-known to form sulfur-bridged complexes.[22]

Concluding Comments. Although several studies have previously addressed the bent metallocene Cp_2ML_x structural questions, the series reported here is particularly engaging in that it is the first to use the same metal–ligand system throughout two modifications: d-electron count change and heterobimetallic bond formation. Most notable about the crystal structures reported herein is the very large ∠S–Nb–S angle change (~25°) upon d-orbital occupancy change in the monomers $Cp_2Nb(SPh)_2$ and $Cp_2Nb(SPh)_2^+$. Since the latter angle of 101.4(1)° is consistent with the ∠S–Ti–S in $Cp_2Ti(SPh)_2$ of 99.3 (3)° and relatively close to all other ∠X–M–X in analogous d^0 complexes, we conclude the ∠S–Nb–S of 75 (1)° in $Cp_2Nb(SPh)_2$ is abnormally small.

A contributing factor to this small angle could be some S···S bonding character, C, since that distance is found to be 3.08 (3) Å average in $Cp_2Nb(SPh)_2$. [In this connection the reported evolution of Ph_2S_2 from $Cp_2V(SPh)_2$ under vacuum is of interest.[4]]

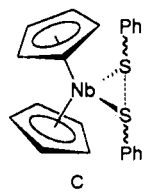

C

The electrochemical analyses of the $Cp_2Nb(SPh)_2$ and $Cp_2Nb(SPh)_2^+$ complexes indicate an accessible Nb(III) oxidation state in stable complex, initially presumed to be the anion of eq 4. The reversibility of this electrochemical wave is prompting further lab bench synthetic efforts. Preliminary results suggest the Na^0/naphthalene reducing agent produces an unstable diamagnetic anion.

$$Cp_2Nb(SPh)_2^+ \underset{}{\overset{-0.29\ V}{\rightleftharpoons}} Cp_2Nb(SPh)_2 \overset{-1.15\ V}{\rightleftharpoons} Cp_2Nb(SPh)_2^- \quad (4)$$
(presumed)

$$Cp_2Nb(\mu\text{-}SPh)_2M^+ \overset{-0.32\ V}{\rightleftharpoons} Cp_2Nb(\mu\text{-}SPh)_2M \overset{-0.70\ V}{\rightleftharpoons} Cp_2Nb(\mu\text{-}SPh)_2M^- \quad (5)$$
(presumed)

M = $Mo(CO)_4$

Equation 5 summarizes the electrochemical data for the heterobimetallic. Whereas the first potential of **4** is at the

exact same value as the Nb(V) → Nb(IV) reduction in the monomeric $Cp_2Nb(SPh)_2^+$, addition of the second electron is considerably easier in the heterobimetallic. In the absence of isolated products and detailed molecular orbital calculations one cannot account for this discrepancy. The gross interpretation, assuming the product are as formulated in eq 4 and 5, is that electron delocalization over two metal centers stabilizes the negative charge of the product anion.

Electron delocalization in the heterobimetallic is effected by bridging thiolate ligands as well as a metal–metal interaction. The latter is implicated not only by the short contact Mo···Nb distance of 3.12 Å from X-ray studies but also by the NMR probe. Noted earlier in the case of isoelectronic $Cp_2Ti(\mu\text{-}SR)_2Mo(CO)_4$ was greater shielding of the Cp protons in the heterobimetallic as compared to the free ligand $Cp_2Ti(SR)_2$.[14] Similarly the Cp protons of $Cp_2Nb(SPh)_2^+$ (at 6.66 ppm) are shifted upfield upon coordination to $Mo(CO)_4$ (δ(Cp) = 5.77 ppm).

A similar conclusion of Mo→Ti interaction was based on a comparison of ν(CO) IR data for $Cp_2Ti(\mu\text{-}SPh)_2Mo(CO)_4$ (ν(CO) = 2018, 1930, 1912, 1899 cm^{-1}) vs $[PhSCH_2CH_2SPh]Mo(CO)_4$ (ν(CO) = 2027, 1905, 1870 cm^{-1}).[18] That there is less electron density on Mo in our cationic complex $Cp_2Nb(\mu\text{-}SPh)_2Mo(CO)_4^+$ as compared to the isoelectronic neutral species $Cp_2Ti(\mu\text{-}SPh)_2Mo(CO)_4$ is clear from the much higher ν(CO) band positions of the former (2058, 1994, 1986, and 1945 cm^{-1}). Whether this is due to a poorer donating ability of the μ-SPh groups or a stronger Mo:→Nb interaction cannot be distinguished.

Of the three resonance forms that have been used to describe the bonding in such heterobimetallics involving bent metallocenyls as ligands,[18,23] we expect the major contributor to **4** to be F, i.e., involving a Mo-donor→Nb-acceptor interaction. That the ∠S–Nb–S changes so little from the free ligand **2** (101.4 (1)°) to the bimetallic **4** (103.1 (1)°) can be attributed to a balance of molybdenum donor→niobium acceptor interaction, partially occupying the $2a_1$ orbital on Nb in the bent metallocene, and the chelating ligand bite angle requirement of Mo. Additional structural studies of the known neutral bimetallic **3** and

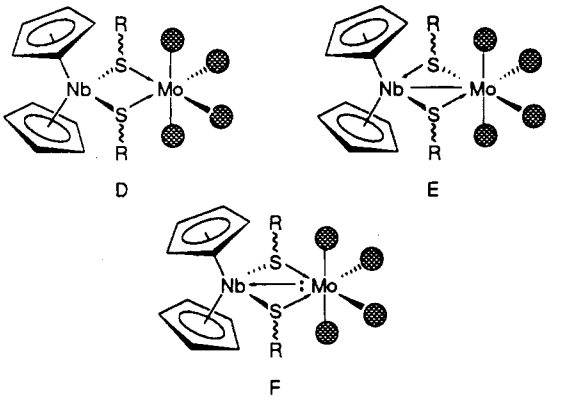

the (presumed) anionic bimetallic implied from the electrochemical results are warranted.

Acknowledgment. The financial support of this research by the National Science Foundation (Grant CHE 86-03664) and Texas A&M University is greatly appreciated. The Nicolet R3m/v X-ray diffractometer and the crystallographic computing system in the single-crystal X-ray diffraction laboratory at Texas A&M University were purchased with funds provided by the National Science Foundation (Grant CHE-8513273). Funds from a NSF Grant CHE-870567 also permitted purchase of the mass spectrometer used in this study. R.S. was recipient of a Brazilian Government Fellowship, CNPq, from the Universidade Federal de Minas Gerais. We gratefully acknowledge helpful discussions with Professors C. Martin and D. J. Darensbourg. The scientific assistance of Dr. Magdalena Pala, Dr. Thomas Sharp, and Viji Dandapani as well as the technical assistance of Monika Frausto in the preparation of this manuscript is acknowledged with gratitude.

Supplementary Material Available: Tables of bond lengths and angles, anisotropic thermal parameters, and hydrogen atom coordinates and packing diagrams for **1**, **2**, and **4** (16 pages); listings of structure factor amplitudes for **1**, **2**, and **4** (52 pages). Ordering information is given on any current masthead page.